Anisotropic colloidal particles near boundaries

Cite as: J. Appl. Phys. **131**, 150903 (2022); https://doi.org/10.1063/5.0089206
Submitted: 23 February 2022 • Accepted: 30 March 2022 • Published Online: 19 April 2022

Journal of Applied Physics

PERSPECTIVE

scitation.org/journal/jap

Jiarui Yan and Christopher L. Wirth

Journal of Applied Physics **131**, 151101 (2022); https://doi.org/10.1063/5.0088214

Journal of Applied Physics PERSPECTIVE scitation.org/journal/jap

Anisotropic colloidal particles near boundaries

Cite as: J. Appl. Phys. 131, 150903 (2022); doi: 10.1063/5.0089206
Submitted: 23 February 2022 · Accepted: 30 March 2022 ·
Published Online: 19 April 2022

Jiarui Yan[1,2] and Christopher L. Wirth[2,a)]

AFFILIATIONS

[1] Department of Chemical and Biomedical Engineering, Washkewicz College of Engineering, Cleveland State University, Cleveland, Ohio 44115, USA [2] Department of Chemical and Biomolecular Engineering, Case School of Engineering, Case Western Reserve University, Cleveland, Ohio 44106, USA

[a)]Author to whom correspondence should be addressed: wirth@case.edu

ABSTRACT

Anisotropic colloidal particles are regularly found in applications ranging from health to energy. These particles, typically with non-uniform shape or surface chemistry, interact with boundaries in unique ways, offering pathways to complex assemblies and active systems. Work in this field over the past two decades rapidly advanced, with the last five years seeing significant innovation. One common thread joining many studies and applications is that of the presence of boundaries in the form of a nearby wall or neighboring particle. Asymmetry introduced by a neighboring boundary often leads to unique and surprising particle dynamics from the resulting anisotropic surface interactions. Herein, we provide background for the area, some recent distinctive examples, and describe recent work from our group developing a technique to measure surface interactions of anisotropic particles. Note that we focused on anisotropic "colloidal" particles with the size ranging from 0.1 to 10 μm in the presence of externally or internally generated fields. Within this context, we then motivate and describe recent work from our group developing an ultra-microscopy technique called Scattering Morphology Resolved Total Internal Reflection Microscopy. Finally, we finish the perspective article by identifying challenges and providing an outlook for the field.

I. INTRODUCTION

Nano- to microscale "colloidal" particles are regularly found as key components in industrial and biological applications (see Fig. 1).[1–10] The size domain occupied by these particles, that of 0.1–10 μm, results in a large surface area to volume ratio that makes a wide range of surface and body forces relevant to the dynamics of these systems. Both surface forces mediated by the physiochemical properties of the particle and continuous phase and body forces mediated by the particle's composition and external fields are relevant when considering particles in this size range. Dispersal of solid colloidal particles in a viscous liquid, such as water, further leads to non-conservative (i.e., path dependent) forces being relevant. The complex interplay of forces engenders a wide range of dynamics in colloidal suspensions. Consequently, field mediated assembly and dynamics of colloids have been a robust field of study for many decades.[11] This perspective aims to first provide historical context to the area, to describe key advances of current work, to identify existing challenges and describe new innovations from our lab in response, and to provide an outlook framed by three important aspects, namely, the variety and nature of fields, the anisotropy of particles, and the presence of boundaries.

Electric,[12–17] magnetic,[18–22] chemical,[23–25] thermal,[26–28] acoustic,[29–31] and hydrodynamic fields[32–34] have been successfully used to drive the motion of individual or assemble ensembles of isotropic colloidal particles. One classic example is that of electrophoresis, which will occur when a colloidal particle with bound charge and associated diffuse layer, forming an electric double layer, is exposed to an external electric field.[35] The electric field acts on the mobile ions in the diffuse part of the electric double layer of the particle to drive its surrounding flow. The particle itself is then driven in the opposite direction in response to the "tank treading" action of the enveloping flow. Other classic examples include dielectrophoresis, in which a particle moves in response to a gradient in the electric field, and magnetophoresis, in which a magnetizable particle moves in response to a gradient in a magnetic field.[36]

One well-studied example of assembly is that of an ensemble of colloidal particles responding to a nearby polarized electrode.[15,37,38] Particles assemble in response to electric field mediated flows driven along the particle surface and electrode boundary.

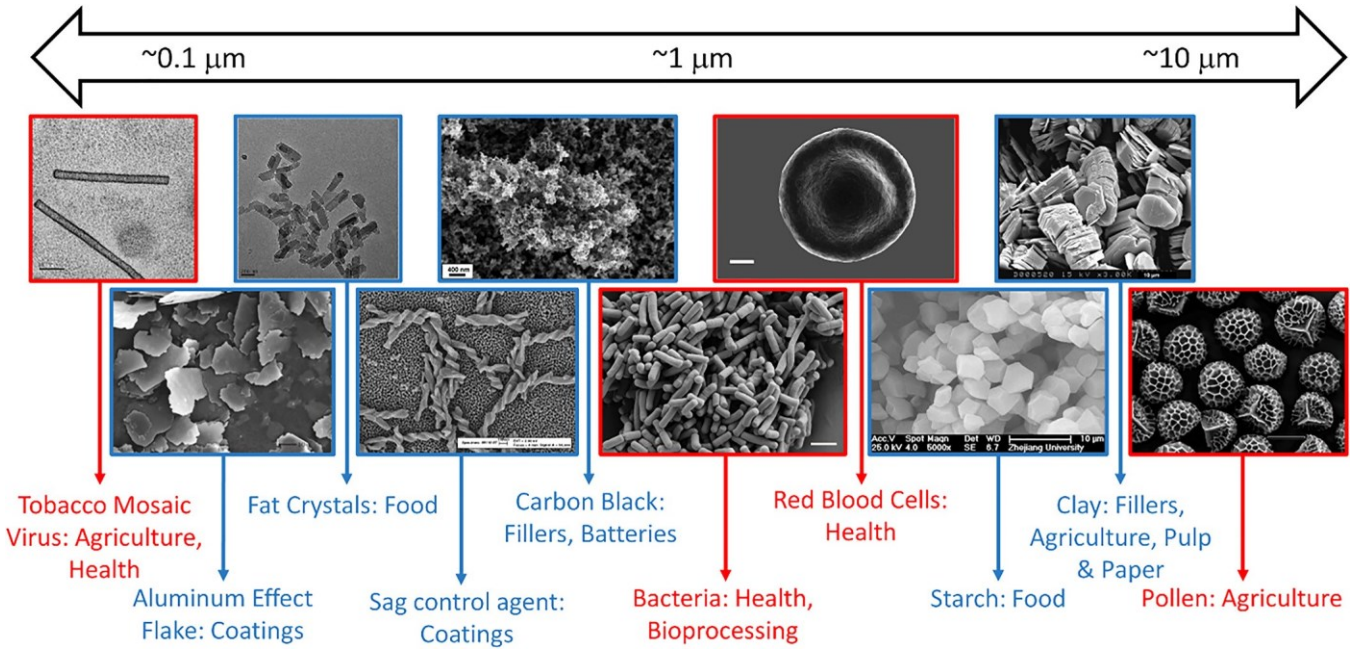

FIG. 1. Anisotropic colloidal particles found in applications across health, agriculture, coatings, food, batteries, and bioprocessing. There is a large variety of anisotropy found among particles with a characteristic size between 0.1 and 10 µm. Anisotropies arise in shape, surface chemistry, and contour, leading to surface forces that depend on not only separation distance but also orientation.[1–10] Reprinted with permission from Qi et al., Prog. Org. Coatings 63, 345–351 (2008). Copyright 2008 Elsevier. Reprinted with permission from Co and Marangoni, Adv. Colloid Interface Sci. 273, 102035 (2019). Copyright 2019 Elsevier. Reprinted with permission from Bosma et al., Prog. Org. Coatings 55, 97–104 (2006). Copyright 2006 Elsevier. Reprinted (adapted) with permission from Ferraro et al., Energy Fuels 30, 9859 (2016). Copyright 2016 American Chemical Society and Buys et al., Cardiovasc. Diabetol. 12, 25 (2013). Copyright 2013 Author(s), licensed under a Creative Commons Attribution (CC BY) license. Reprinted with permission from Sun, X.-B. Zuo, S. Fang, H.-N. Xu, J. Chen, Y.-C. Meng, and T. Chen, J. Texture Stud. 48, 241–248 (2017). Copyright 2016 John Wiley and Sons. Reprinted with permission from Wilson, L. Wilson, and I. Patey, Clay Miner. 49, 147–164 (2014). Copyright 2018 Cambridge University Press. Reprinted (adapted) with permission from Binks et al., Langmuir 21, 8161–8167 (2005). Copyright 2015 American Chemical Society.

Similar processes can also be driven by electric fields in 3D.[39] Application of these processes ranges from fabricating colloidal crystals for photonic materials to that of electrorheological fluids in which particles are driven to form chains that will significantly alter the rheological properties of the continuous phase. Similarly, magnetic fields have been used to drive the dynamics of individual particles, as well as assemble ensembles into chains, 2D, and 3D.[40,41] Applications of these processes are quite broad because of the robustness of using a magnetic field, which avoids certain problematic features, such as electrochemical reactions, often encountered with electric fields. Note also that although electric field driven processes occur via both surface mediated and body forces, magnetic field driven assembly processes are typically driven by body forces.

Other types of fields have also been widely adopted to control the dynamics of colloidal particles. As discovered nearly 50 years ago, gradients in chemical or thermal fields will drive particle motion. An isotropic colloidal particle will be driven to "swim" in response to an imposed gradient of solute via diffusiophoresis,[23] while a similar process will occur in a thermal gradient via thermophoresis.[42,43] These physiochemical phenomena have found new appreciation over the past 15 years as anisotropic particles have been designed and synthesized to generate local gradients that facilitate transport. Acoustic streaming fields[31] or hydrodynamic fields (i.e., the flow field associated with the continuous fluid) are yet another set of mechanisms to which colloidal particles will respond.[44]

Recently, there has been an increased emphasis on the role anisotropy may play in the broad set of phenomena described above. This renewed emphasis arises from both the recognition of the wide array of anisotropies encountered in applications and the successful pursuit of new fabrication methods for anisotropic colloidal particles.[45] Anisotropy can generally be thought of as a particle feature that imparts a difference from that of a sphere of uniform composition, surface chemistry, and mechanical properties. Figure 1 illustrates the large array of anisotropic particles found in applications ranging from Health, Agriculture, Food, Pulp & Paper, Batteries, and Coatings. Note the large variety of anisotropies. Particles may have aspect ratios differing from one that are either prolate or oblate, have a cavity or be dimpled, or have a swirling contour or be faceted. These particles could also have anisotropy in surface chemistry, composition, mechanical, and electrical

properties. Anisotropic features will play a significant role in the particles' dynamics in response to the various fields noted above. In some cases, an anisotropic feature will respond to the field (e.g., shear alignment of rods[46]), whereas in other cases the anisotropy is necessary to create the field (e.g., catalytic Janus particle[47]). While the former plays a significant role in many industrial applications, for instance, the pumping of a suspension of fibers,[48] the latter has been identified as a model analog system for biological entities.[49]

The third element of emphasis in this perspective is that of boundaries. Particles are regularly found near boundaries or in crowds. For instance, red blood cells interact with boundaries or neighbors either in the body or in a diagnostic device.[50] These interactions play an important role in the proper function and health of the vasculature. Abnormal surface interactions can be an indication of a disease and cause significant damage.[51,52] Thus, an appropriate understanding of these interactions is of significance in that boundaries introduce both conservative and non-conservative interactions via the surface chemistry and hydrodynamic interactions, respectively. Anisotropies will tend to further make these interactions asymmetrical to the extent that particles will behave in unique and potentially useful ways.

This perspective is organized as follows. First, relevant classes of anisotropy are described along with the recent advances in fabrication methods used to make particles. Next, a selection of fields will be described relevant to the dynamics of anisotropic colloidal particles. Those fields are organized into "external" and "internal" fields, in which the former can be considered imposed fields, while the latter are fields generated by the particle itself. This section focuses on the application of these phenomena near boundaries. We will then explore recent innovations for measuring the dynamics of anisotropic particles near boundaries, with a particular emphasis on Scattering Morphology Resolved Total Internal Reflection Microscopy (SMR-TIRM). Finally, Sec. V identifies a selection of challenges and opportunities in this area. It is important to note that there is a substantial amount of related work that is outside the scope of this perspective. Herein, we focus on solid colloidal particles with a characteristic size between 0.1 and 10 μm. There is a large body of literature focused on anisotropic nanoparticles[53] and liquid crystals[54] for which many synthetic routes exist.

II. ANISOTROPIC PARTICLE DESIGN AND FABRICATION

A. Geometric anisotropy via mechanical methods

A particle is typically considered to be geometrically anisotropic when its shape differs from a sphere, but this guideline could be generalized to a particle with a variation in curvature along its surface as anisotropic. Rough or faceted particles with local curvature variations are often considered anisotropic and have recently been explored.[55] Prolate and oblate ellipsoids,[56] dumbbells,[57] snowmen,[58] and bowls[59] are all examples of colloidal particles with anisotropy in shape that have been successfully fabricated (see Fig. 2). A large selection of fabrication methods can be organized into categories of mechanical manipulation, controlled aggregation, printing, and synthetic routes.

Mechanical manipulation techniques typically rely on a spherical polymer particle being dispersed in a film, heated to above the glass transition temperature of the polymer, mechanically manipulated via uniaxial or biaxial stretching, and then thermally quenched to make permanent the new shape.[60] This technique is particularly well-suited for adjusting the aspect ratio of particles to make either prolate or oblate ellipsoids. Some key advantages of this technique include the ease with which the aspect ratio can be adjusted, the capability to produce large quantities of particles, the ability to utilize polymer particles with fluorescent tags, and the relatively wellcontrolled dispersity of product. Although initially developed nearly three decades ago, progress has been made in developing precise and scalable methods for fabricating prolate ellipsoids in recent years. Motivation for these advances resides primarily in the need for sufficient material to operate at semi- to concentrated regimes in rheology and colloidal assembly processes.[61–65] These updated fabrication routes are excellent improvements in precision and scalability of the film stretching technique.

First, a two-step continuous film stretching process was recently developed capable of producing up to ~1 g of monodisperse prolate ellipsoids, more than 20 times the typical production rate of batch processes.[66] The team utilized existing polymer processing steps, such as draw down (to fabricate the film) and roll-to-roll (to facilitate fabricating the film), to achieve continuous film production, flash, and stretching. This advance facilitates long continuous runs of film to be processed to produce monodisperse samples (see Fig. 3). Even more recently, another variation of the mechanical manipulation process was developed in which a film was stretched with a gradient such that samples of ellipsoids with systematic variation in the aspect ratio could be reliably generated from a single film.[67] The authors were able to convincingly show that a film stretched in this fashion would yield a wide selection of aspect ratios. Although this technique has yet to be made

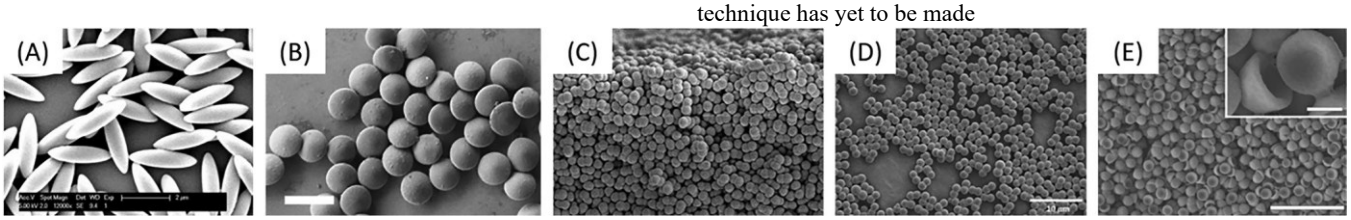

FIG. 2. Small selection of shape anisotropic colloids that include (a) prolate ellipsoids, (b) oblate ellipsoids, (c) dumbbells, (d) snowmen, and (e) bowls.[56,57,59,185,186] Reprinted (adapted) with permission from Coertjens et al., Langmuir 33, 2689 (2017). Copyright 2017 American Chemical Society.

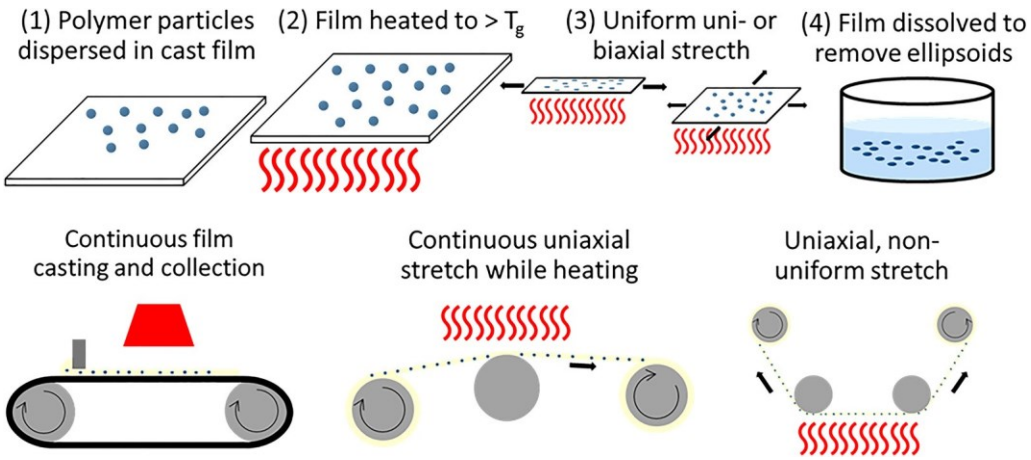

FIG. 3. Mechanical manipulation for shape anisotropic particle fabrication. The original technique consisted of (1) dispersion of polystyrene spheres into and batch casting of a polyvinyl alcohol film, (2) batch heating of the film to above the glass transition temperature, (3) uniform stretching along one (uniaxial) or two (biaxial) directions, and finally (4) dissolution of the film to suspend the ellipsoids. Recent advances include that of dispersion and continuous casting of the film, continuous uniform uniaxial stretching of the film, and batch uniaxial, but non-uniform stretching of the film. These advances allow for the fabrication of either large quantities or large distributions of an aspect ratio of shape anisotropic particles.[66,67]

continuous, it is quite useful for the rapid production of many different aspect ratios of ellipsoids (see Fig. 3).

In general, challenges with mechanical manipulation techniques mainly center on material choice and hardware. Suitable material choice for a particle has so far been restricted to those with a glass transition temperature (i.e., polymeric) and are most often polystyrene or poly(methylmethacrylate) (PMMA).[68] Further, the particle should be compatible with the continuous film in which stretching occurs. Another challenge with this technique is that of hardware. Most apparatus for conducting such stretching processes are either small custom-built machines or very large, commercial grade biaxial stretchers. The former takes time to build and typically is small, thereby limiting throughput, whereas commercial biaxial stretchers are not common in university settings. There remain few economical, commercial options for biaxial stretching with controlled temperature.

B. Geometric anisotropy via chemical routes

In addition to mechanical methods, there are a variety of chemical routes to produce geometrically anisotropic particles. For instance, one class of techniques to control shape consists of using building block "base units" in conjunction with a controlled aggregation process. Such processes typically consist of spherical particles of different sizes that are induced to flocculate via rapid changes in salinity or some specific chemical binding mechanism. For example, one route for the fabrication of doublets entails mixing suspensions of like charged particles along with a high concentration of electrolyte.[69] Flocculation is allowed to proceed for some period before the process is quenched by diluting the suspension with ultra-pure water. Related techniques are those that use the covalent attachment of particles or droplets with specific or non-specific interactions.[70–72] Both processes, that of flocculation and chemical bonding, typically result in anisotropic particles that appear as doublets, snowmen, or bumpy.

One effective technique for fabricating colloidal particles with anisotropy in both shape and chemistry is that of seeded polymerization and swelling.[73–75] Initially developed 30 years ago, this particle fabrication technique has recently been adopted to fabricate doublets with a systematically different size and chemistry.[76–78] Anisotropic particles are fabricated by starting with a crosslinked polymer sphere that is exposed to monomer. The monomer tends to swell the polymer sphere on a very short time scale, followed by separation to produce a small bulb on the surface that is subsequently polymerized at elevated temperature. The resulting anisotropic particle can then be further modified to have lobes of different chemistry. Further, there are other synthetic routes for producing rod-like particles with excellent control over aspect ratios.[79,80] Aspect ratios ranging from ~1 to 25 were achieved, with the width of these silica rods roughly 200 nm.

Note that these bottom-up techniques to fabricate geometrically anisotropic particles are complemented by an array of top-down techniques primarily based on photolithographic printing.[81] Recent studies[82,83] using similar top-down techniques showed that optically assisted printing of a colloidal scale particle with a complex geometry was possible. Exquisite geometry on the nano- to microscale is possible with this technique, varying aspect ratios, faceted, or looping structures have all been achieved. Despite being somewhat limited in particle fabrication throughput, this approach offers excellent precision in the nanoscale resolution of the shape and structure of particles.

C. Chemical anisotropy

Another avenue in which anisotropy may be introduced into a particle system is that of surface chemistry. Many colloidal particles found in real applications, such as filler clays or pigments for coatings, will display chemical anisotropy in addition to shape anisotropy. Three avenues by which particles can be made chemically anisotropic include Glancing Angle Deposition (GLAD), chemical modification via interfacial pinning, and synthetic routes.

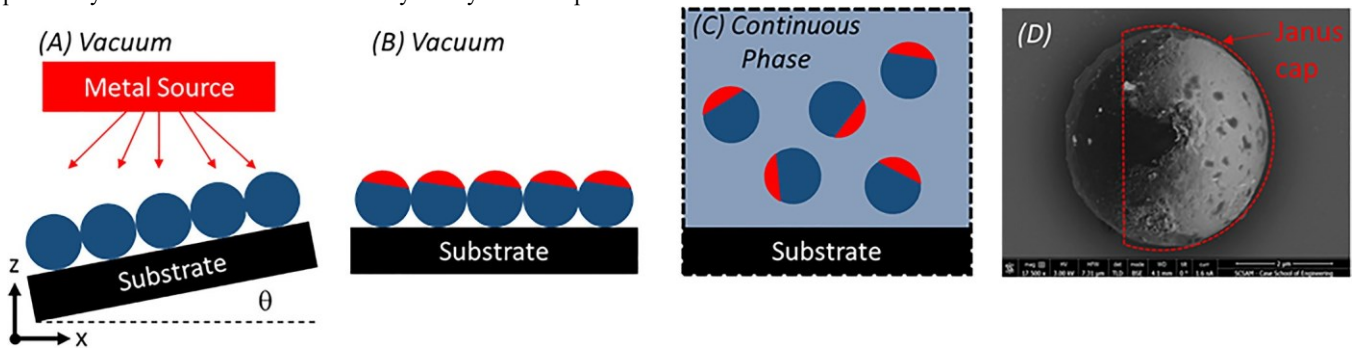

FIG. 4. Glancing Angle Deposition (GLAD) Fabrication Process. (a) A monolayer of particles at angle θ is exposed to some metal source in vacuum. (b) Systematic adjustment of θ alters the cap coverage. (c) Those particles can then be released into solution. (d) SEM imaging of a Janus particle with gold cap, revealing the roughened nature of the cap.

Since its invention in 1997,[84–86] GLAD has become a technique of choice for fabricating patchy colloidal particles.[87–90] Briefly, GLAD consists of using physical vapor deposition or sputtering to deposit a layer of a material on a monolayer of colloidal particles (see Fig. 4). Material is deposited on the exposed surface area of a monolayer of particles situated perpendicular to the source. When conducted with the substrate perpendicular to the source, GLAD typically yields particles with one coated hemisphere, i.e., "Janus" particles. Systematic adjustment of the substrate inclination angle θ or the angle of crystallinity with respect to the source impacts the patch coverage as well as shape. Metals, such as platinum, titanium, and chrome, are often the deposition material of choice in GLAD, but other materials, such as carbon, have also been employed.[91] Although there is some restriction with respect to chemistry for the deposited layer, one significant benefit of this technique is that there are very few restrictions on the chemistry of the native particle. The only requirement for the native colloidal particle is that a relatively uniform monolayer of that particle must be achievable. One engineering challenge with this technique is that of scalability. There remain some limitations on the quantity of material that can be made with this method, primarily because monolayers are typically processed on wafers that do not exceed a few ~in^2. However, in principle, there is no limit on such a technique if continuous monolayers can be fabricated and subsequently modified via physical vapor deposition.

A second technique well suited to fabricating Janus particles is that of chemical modification during interfacial pinning.[92–95] This fabrication process consists of first pinning native colloidal particles at a fluid/fluid interface, typically as a Pickering–Ramsden emulsion, and then selectively modifying one side of the particle via the continuous phase. Another variation on this technique is solidifying one phase to lock-in the positioning of the cap boundary. Solidifying the non-modifying phase would also help to eliminate the possibility of solute diffusion into that phase. Although there are some material limitations to this technique because of the requirement to first prepare a Pickering–Ramsden emulsion, this avenue does offer increased flexibility, in comparison to GLAD, for material choice of the cap. An additional strong point for this technique is that of scalability. Processing occurs in a volume, facilitating the fabrication of many more particles as compared to most examples of GLAD. However, GLAD at this point offers more control of specific geometry (i.e., patch size and shape).

As is the case for shape anisotropy, there exist synthetic routes for preparing colloidal particles with chemical anisotropy. For instance, there have been multiple examples of molecularly thin, 2D nanosheets being chemically modified such that each side of the individual sheets has distinct chemistries. Graphene oxide (GO) has been modified in this fashion by using a Pickering–Ramsden templating technique.[95,96] In both cases, the GO sheets were first adsorbed onto an interface of a wax-in-water emulsion such that one side of the GO was exposed. Subsequent steps utilized aqueous phase chemistry to chemically modify the exposed GO face. One

such route utilized poly(propylene glycol) bis(2-aminopropyl ether) as chemical modification, while another polymerized methyl methacrylate onto the exposed GO face. A mix of chemical analysis and physical measurement techniques have been employed to verify the asymmetric chemistry. For instance, both FTIR and XRD were used to verify via chemical analysis, whereas analysis of surface pressure isotherms has been used to infer the presence of asymmetric chemistry.

Some of the fabrication routes described above are amenable to serial processing, facilitating the combination of geometrical and chemical anisotropies. One excellent example is that of uniaxial stretching and GLAD. Previous work has shown that combining these processing steps in serial will result in fascinating and useful anisotropic colloidal particles. Moreover, the order in which the processing steps occurred strongly influenced the final function of those particles. In one study, polystyrene particles with a florescent tag were first made Janus, with a gold cap covering roughly 50% of the native particle, and subsequently uniaxially stretched. Processing particles in this order resulted in "Janus Kayaks," essentially particles that had half an ellipsoid as defined along the long axis, with a small spherical cap.[97,98] Changing the order of these steps, with stretching occurring before GLAD, resulted in ellipsoid particles in which one half was coated with gold.

Combining anisotropy of both shape and chemistry in these particles led to distinctly different assemblies in the absence of external fields. Assembly structure was sensitive to the concentration of the electrolyte in the continuous phase. At low to intermediate salt concentrations (2.5 mM NaCl), the "Janus kayak" particles were found to preferentially assemble in structures that maximized gold–gold contacts. Those structures that maximized these contacts tended to be more ordered, in comparison to assemblies obtained at large salt concentrations (100 mM NaCl). Optimal screening of electrostatic repulsion, such that gold–gold is attractive while gold–polystyrene remains repulsive, is the origin of these unique structures. Subsequent work demonstrated the response of the assembled structures to external fields. Ordered ellipsoid fibers, assembled from Janus ellipsoids with gold patches facing each other, were shown to expand and contract in response to an external electric field being toggled on and off, respectively. The actuation of a fiber in this fashion has the potential to serve as an analog to muscle fibers.

Very recent work in this area revealed a unique response of Janus ellipsoids with complex patches in response to AC electric fields.[99] Helical trajectories were achieved by driving Janus ellipsoids with patches of complex shape. Such patches were achieved by conducting glancing angle deposition not only on monolayers of ellipsoids but also on multilayers of ellipsoids in which parts of the patch were shadowed by other layers. In the presence of an AC electric field, the asymmetric patches induce asymmetric induced charge electrophoretic (ICEP) motion that results in helical trajectories depending on the asymmetry. These excellent examples reveal the potential to produce complex trajectories when combining anisotropies in shape and surface chemistry when the particle responds to an electric field.

III. PARTICLES INTERACTING WITH FIELDS NEAR BOUNDARIES

A. External fields

A variety of external fields have been used for decades to modulate the dynamics of colloids, including electric, magnetic, thermal, and hydrodynamic fields. Electric fields are used to drive motion or assemble ensembles of particles via application normal to or perpendicular to the boundary. Historically, a significant chunk of work focused on isotropic particles that formed 2D assemblies, while more recent work utilizes the same electrode geometry to modulate the dynamics and assembly of anisotropic particles.[13,17,100–109] The typical experimental setup consists of parallel plate electrodes spaced ∼100 to ∼1000 μm apart polarized with either steady (DC) or oscillatory (AC) potential. This electrode arrangement generates an electric field nominally normal to the boundary that produces electric field mediated flow along the electrode and particle surfaces. The origin of the flows is the action of the electric field on both induced and equilibrium charges on the relevant electrode and particle surfaces. The electric field mediated flow will cause neighboring isotropic particles to assemble into ordered structures.

Both chemically and geometrically anisotropic particles have been found to generate flow fields with broken symmetry in response to an electric field when near a boundary.[109–111] Initial work tended to focus on induced charge electroosmotic (ICEO) mechanisms, in which the electric field drove the motion of a Janus particle situated near a nonconducting boundary.[110–112] More recent work focused on propulsion and assembly driven by electrohydrodynamic (EHD) and electrokinetic (EK) flow fields with broken symmetry introduced by the anisotropic particle [see Fig. 5(a)]. Note that these mechanisms were extensively studied in earlier works with either isotropic particles or planar interfaces, with those contributions showing how each mechanism scales with the electric field strength and frequency. The electrode geometry (e.g., parallel vs co-planar) or physiochemical features of the particle (e.g., conducting vs non-conductivity) may impact the relative strength of various mechanisms. Yet in general, equilibrium charge mechanisms, which typically scale linearly in the electric field $\sim E$ (e.g., electroosmosis), are thought to be important in low-frequency electric fields, whereas induced charge and dielectrophoretic mechanisms, which scale to the square of the electric field $\sim E^2$, tend to be important at intermediate or larger electric field frequencies.[113–115] Flow fields with broken symmetry about the axis perpendicular to the boundary induce assembly or propulsion at sufficiently high or low particle concentrations, respectively. Neither propulsion nor complex assemblies would be possible with isotropic particles interacting via isotropic interactions. The key for tailoring these interactions is to adjust the relative surface charge (in the case of chemically anisotropic) or the lobes (in the case of geometrically anisotropic) such that the magnitude and direction of the flow fields can be tuned.[105]

A significant amount of related work has explored the response of anisotropic colloids to a magnetic field. One useful feature of magnetic fields is that complex structures can feasibly be fabricated for both isotropic particles[19,20,40,116–118] and anisotropic particles with steady or time varying magnetic fields[119] [see Figs. 5(b) and 5(c)].

Moreover, the variety of mechanisms by which particles assemble tends to be smaller for magnetic fields in comparison to electric fields. Efforts in this area have shown, for instance, that Janus particles with a shifted magnetic dipole can induce unique assembly structures.[22,120,121] Beyond Janus particles, there are also excellent examples of patchy magnetic cubes that assemble into controllable chains.[122,123] Both examples, chaining of Janus spheres and cubes in response to a magnetic field, serve as potential building blocks for a growing field of microrobots.[124,125] Magnetic field actuation has significant potential in this area because of both the controllable nature of the external field and the lack of reaction products that would typically be associated with electric field mediated processes. Finally, note that the acoustic field power by ultrasound at a proper frequency could also be used to drive anisotropic particles, such as gold microrods. Due to the anisotropy in the geometry of microrods, the localized acoustic streaming would induce torques and force the microrods orbiting and spinning.[31] Besides, the gold microrods could further be modified with Fe_3O_4 nanoparticles to become applicable in extensive biological environments.[29]

B. Internal fields

Work on the related phenomena of particle propulsion and assembly driven by internal fields has grown rapidly over the last 10 years.[49,126] Typically, internal fields, or those fields generated by the particle itself, are associated with diffusiophoretic motion from a local reaction or demixing. This definition could be broadened to include some of the work described above on anisotropic particles that generate asymmetrical flow fields in response to an externally applied field. Diffusiophoretic motion can be generated by inducing gradients in solute on the scale of the particle. Gradients in solute are most often achieved via either a catalytic reaction or local demixing. The classic catalytic active particle is that of a Janus sphere or rod with a platinum cap dispersed in a solution of hydrogen peroxide.[127–129] Platinum catalyzes a reaction with hydrogen peroxide that results in solute gradients across the length scale of the particle. For cases with an insulating native particle, motion is driven up or down this gradient because of self-diffusiophoresis. In systems with a conducting native particle, for example, a gold rod coated with a cap of platinum in the presence of hydrogen peroxide, the mechanism is thought to be self-electrophoresis. Particle propulsion arises from the self-generated local electric field. Recent work has shown that catalytic active particles that are crowded, either near a wall or a neighbor, experience a chemotactic response that will further complement this motion.[130]

The second example of solute driven propulsion is that of a chemically anisotropic particle swimming in response to the demixing of a critical solution. These systems work by locally heating the cap of a Janus particle suspended in a critical solution

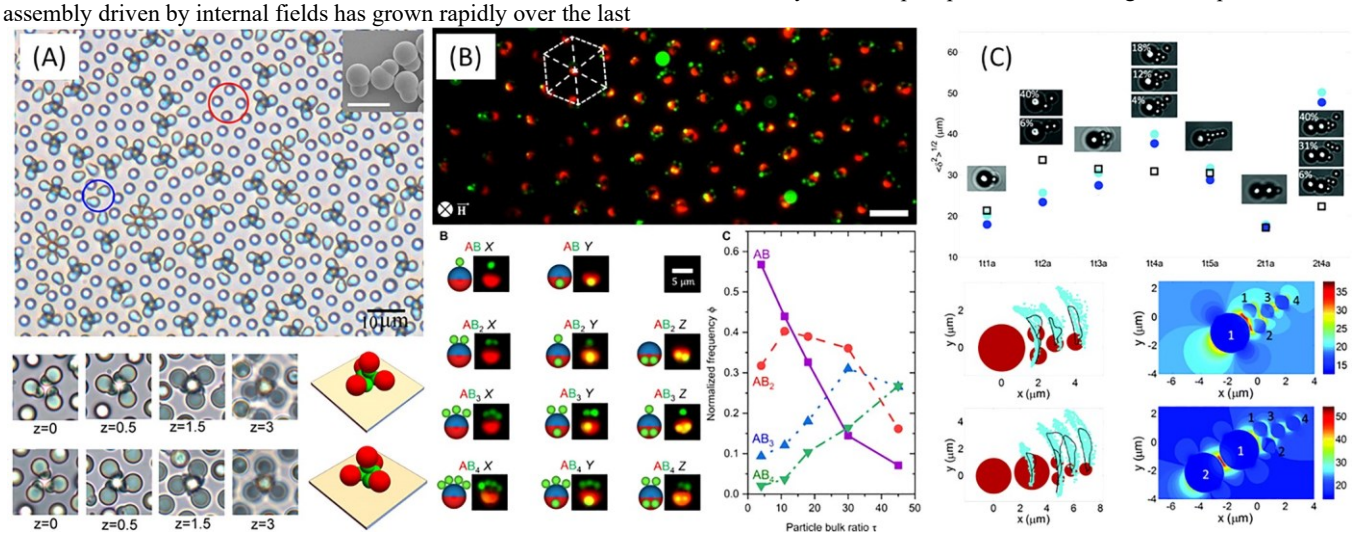

FIG. 5. Electric and magnetic field mediated dynamics of anisotropic particles near boundaries. (a) Chiral colloidal clusters were assembled from asymmetric doublets very near a polarized electrode.[101] The authors found that colloidal doublets experienced asymmetric electrohydrodynamic flow in response to application of an electric field. Neighboring colloidal doublets then assembled into chiral colloidal structures. Reprinted with permission from Ma et al., Proc. Natl. Acad. Sci. 112, 6307 (2015). (b) Colloidal Janus particles consisting of native polystyrene particles and an iron cap respond to a magnetic field in the presence of polystyrene nanoparticles. The magnetic field induces assembly to create unique, asymmetric structures with systematic variation in product stoichiometry depending on the reactant concentration and field frequency.[119] From Al Harraq et al., Sci. Adv. 6, eaba5337 (2020). Copyright 2020, Author(s) licensed under a Creative Commons Attribution (CC BY) license. (c) Superparamagnetic particles of systematically varied diameter were assembled in a rotating magnetic field and then subsequently modulated to generate low-Reynolds number swimming via mechanical means facilitated by the system's asymmetry. Each of these excellent examples reveals how particles are assembled and manipulated to form complex structures or dynamics not possible with isotropic particles.[116] Reprinted with permission from Du et al., Soft Matter 14, 3463 (2018). Copyright 2018 Royal Society of Chemistry.

that demixes at a given temperature.[91,131,132] Silica particles with a carbon cap dispersed in water-lutidine were the original example of such a system, but other examples include spherical silica particles and geometrically anisotropic SU8 particles with gold caps. A focused light source with a wavelength at which carbon absorbs was used to heat the solution on the scale of the particle. Demixing then creates a solute gradient that drives particle propulsion. Additionally, there are other examples of light activated particles.[133]

Perhaps, the most significant set of innovations over the last 5 years has been in the combination of these strategies to actuate motion on the microscale.[108,134–139] In one example, a surfactant aided dewetting process was used to produce lobed particles that had both chemical and geometric anisotropy.[136] Interestingly, the authors were able to synthesize particles with multiple lobes that could be located at different angles with respect to each other. Further, although the primary particle and lobes are insulating, the lobes themselves are then modified with gold. When placed in a low-frequency AC electric field, the lobes generated induced charge flow because of the mismatch in electric properties, but also depended on the orientation of the lobes. For instance, the propulsion velocity depended upon the bond angle between lobes.

Another recent example of combining multiple anisotropies to produce controllable motion is that of new responsive microswimmers that adapt to the local environment,[135] thereby replicating those systems found in nature. In this work, a polystyrene (PS) bead is coupled to a temperature response microgel, poly-isopropylacrylamide-co-methacrylic acid (PNIPAM-co-MAA) via capillary assisted particle assembly. The resulting doublet structure then has two components, one of which is a microgel that goes through a volume and electric property transition with a change in temperature and the other (PS) does not. Further, the doublet system propels in response to an externally applied AC field. However, the mobility of the doublet reverses depending on whether the microgel is swollen or compacted. Thus, via a simple local heating of the doublet from a light source, the direction of propulsion can be altered. These two fine examples reveal the potential for combining different strategies in the design of anisotropic particles.

IV. COMPLEX PARTICLES INTERACTING WITH BOUNDARIES

Many studies are motivated by the assembly and propulsion of anisotropic particles near a boundary. For instance, microorganisms, or more broadly biological active particles, are regularly found near a boundary as this is often the first step to some functional process, such as biofilm formation.[140] The presence of a nearby boundary then requires careful consideration of the conservative and non-conservative interactions experienced by individual particles. These interactions can be mediated by external fields or operate in the absence of those fields. There is a long history of predicting and measuring non-conservative particle interactions with a boundary, especially for spherical and near-spherical particles of uniform chemistry.[141–145] These efforts were primarily focused on the hydrodynamic interactions that arise as a micrometer scale particle approaches a boundary at small or zero Reynolds number. Analytical expressions for the translation and rotation of these particles have found broad use in many fields. In addition, conservative interactions that typically arise from electrostatic, van der Waals, steric, or depletion interactions have been measured, along with the impact of these interactions on particle dynamics for some time.[146,147]

More recently, work in this area has broadened to include particles of more complex shape or surface chemistry. For instance, there are now significant efforts in biological particle interactions and adhesion to surfaces because of the importance of these phenomena to biofilm formation and blood flow.[148–154] Recent work has explored the influence of various physiochemical and biological factors on the attachment of Escherichia coli to solid/liquid and liquid/liquid interfaces.[155–157] Although there are some instances in which employing DLVO or DLVO like interactions to describe bacteria adhesion works well, these lack realistic descriptions of the bacteria′s surface and consequently will frequently fail to capture the real phenomena.[158] One example in this area is that of measuring the impact of fimbriation of E. coli on the initial stages of biofilm growth.[157] Fimbriae are long tendril like structures emanating from a bacteria′s surface that are <10 nm in diameter but tend to be ∼100 s nm in length. The authors employed E. coli with differences in the number density of fimbriae expressed on the bacteria′s surface via a gene mutation. Interestingly, although changing the number of fimbriae on the bacteria′s surface did not influence physiochemical features like zeta potential or surface energy, there was a systematic change in the adhesion behavior of the bacteria depending on whether it expressed the fimbriae, thereby demonstrating the importance of including particle complexity in interaction and adhesion analysis. Other interesting examples exist in nature. For instance, recent work found that bacteria could swim upstream as facilitated by boundaries.[159] E. coli were found to propagate long distances in a microfluidic channel against a prevailing flow. These surprising bacterial dynamics are thought to be dictated by the hydrodynamic interactions introduced from the nearby boundaries. Understanding the motion of bacteria benefits the prevention of infections and microbial soil pollution.

Another area in which complex particle interactions with a boundary are relevant is that of red blood cell (RBC) adhesion.[52,160,161] like bacteria adhesion, most experimental methods are, to this point, only able to make binary measures of adhesion with digital video microscopy.[162,163] Yet, the interactions and adhesion of RBCs are known to be far more complex, especially when considering the potential variations in the mechanical properties of a capsule. RBCs are capsules that will deform differently depending on the disease state. For example, sickled RBCs tend to have a stiff morphology that contributes to vasculature blockage. The interactions and adhesion of these cells are not well described by DLVO-like interactions. Rather, recent work has utilized numerical solutions to reveal the complex state diagram of healthy and diseased RBCs near a boundary.[164–166] In one example, a dissipative particle dynamics simulation tool has been employed to predict how RBCs occlude passageways as a function of cell shape and rigidity. These studies have also been paired with microfluidic assays that quantify

the deformability of RBCs with the cell aspect ratio at systematically different shear stresses.

Both examples described above, that of bacteria and red blood cell adhesion, have made significant progress in our understanding of how these complex colloidal particles approach and interact with boundaries. Yet, there remains a dearth of measurement techniques to track the response of these systems to fields, external or otherwise. Most often, colloidal particles in response to a field and near a boundary are tracked with bright-field microscopy, epifluorescence, or confocal microscopy. Existing algorithms for tracking particles are now widely available and implemented,[167–169] but those are most relevant for colloidal particles that are isotropic, tagged, and with tracking in a single plane. A clear need is a technique capable of measuring particle motion in not only the xy-plane, but also normal to a neighboring boundary, in the z-axis. Although confocal microscopy can track motion in the z-axis, the resolution of those measurements is typically insufficient for tracking fine details. In addition, orientation also should be tracked for anisotropic particles. Such tracking can be accomplished with confocal, but only for cases in which the particles have multiple fluorescent tags. Note that the discussion herein is primarily focused on particles very near boundaries, with a separation distance approximately equal to that of a particle diameter. Note also that holographic techniques have advanced now to the point that isotropic and some anisotropic particles can be tracked.[170]

One potential solution to these challenges is that of an ultramicroscopy technique called Total Internal Reflection Microscopy (TIRM).[146,171,172] TIRM relies on an evanescent wave propagating along the substrate neighboring a freely diffusing colloidal particle [see Fig. 6(a)]. The evanescent wave has an intensity that decays exponentially into solution such that the intensity of light scattered by an isotropic particle is exponentially sensitive to changes in the

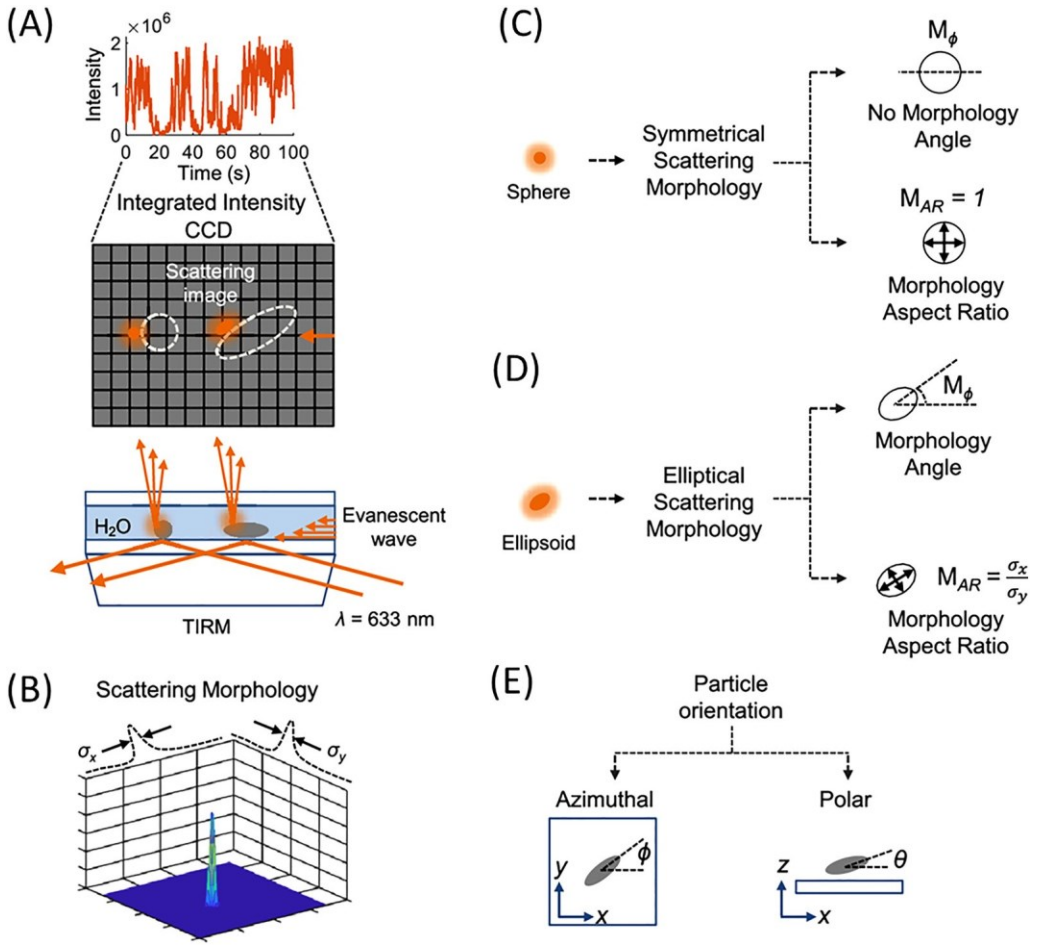

FIG. 6. Essential features of Scattering Morphology Resolved Total Internal Reflection Microscopy (SMR-TIRM). (a) SMR-TIRM works by collecting the morphology of light scattered from particles near a boundary and exposed to an evanescent wave.[174] (b) The morphology of scattered light is fit with a 2D Gaussian function to obtain the angle M_f and aspect ratio M_{AR} of the morphology. (c) and (d) At most conditions, spherical particles produce symmetrical scattering morphology, while ellipsoidal particles produce an elliptical scattering morphology. Note, however, that recent work from our group has shown at what conditions even a spherical particle will have an elliptical scattering morphology.[175] (e) M_f and M_{AR} in principle can be used to independently determine the azimuthal f and polar θ angles of an ellipsoidal particle. Reprinted (adapted) with permission from Rashidi et al., Langmuir 36, 13041 (2020). Copyright 2020 American Chemical Society.

position normal to the boundary. Developed nearly three decades ago, TIRM has continued to be used to track the dynamics of isotropic particles facilitating the measurement of conservative surface interactions. Yet, such a technique as described would not work for an anisotropic particle. The primary challenge in utilizing TIRM for anisotropic particles is that the signal of light scattering is no longer solely dependent on the separation distance between the particle and surface. Rather, the morphology of scattered light depends on not only the separation distance, but also the orientation and, ultimately, the optical anisotropy of a particle. Recently, our group has begun working on solutions to this challenge by developing Scattering Morphology Resolved Total Internal Reflection Microscopy or SMR-TIRM.[173–175] The essence of SMR-TIRM is that the morphology of scattering, rather than the integrated intensity, is used to evaluate the orientation and separation distance of an anisotropic particle. Simulations of the light scattering, and more recent experiments, have shown the morphology of scattering from one model anisotropic particle, a prolate ellipsoid, is an effective reporter of the orientation and separation distance of the particle itself.[174]

The essential concept of SMR-TIRM is in the collection of the scattering morphology, rather than the integrated intensity associated with a particle. The morphology is then parameterized to track the orientation and position of a particle, thereby providing the dynamics of a particle along with a pathway to calculate the potential energy landscape. Scattering is parameterized via fitting a twodimensional (2D) Gaussian to the morphology. The 2D Gaussian yields two important parameters, namely, the morphology angle M_θ and aspect

ratio M_{AR}. The morphology angle is defined as the angle of rotation of the long axis of the morphology, measured counterclockwise from the direction that the evanescent wave propagates. The morphology aspect ratio is defined as the ratio of the long axis and short axis of the 2D Gaussian fit. The integrated intensity is also collected during the image analysis process. Our previous work has shown that M_f is an effective reporter of the particle azimuthal angle, while M_{AR} is an effective reporter of the polar angle of the particle. Moreover, we found the later quantity to be only very weakly dependent on the former; i.e., M_{AR} does not strongly depend on M_f. Consequently, the azimuthal and polar angles can, in principle, be tracked independently. Further, our work has revealed that the integrated intensity remains exponentially dependent on separation distance at a fixed orientation. Thus, each of the quantities defining position—height, azimuthal angle, and polar angle—can in principle be obtained independently.

Initial work in developing SMR-TIRM focused on collecting the scattering morphology from multiple prolate ellipsoids at systematically varied orientation.[174] Although this early experimental work, along with complementary simulations, revealed the qualitative dependence of morphology angle on particle angle, the pathway by which data were collected leads to significant noise in these data. Initially, systematically varied orientation was achieved via deposition of many particles at differing orientations. However, these measurements were quite noisy given that particles would often have slight differences in the aspect ratio, volume, polar angle, or have different locations within the evanescent field. In response to this experimental challenge, we are currently developing a variable azimuthal angle SMR-TIRM (see Fig. 7).

The variable azimuthal angle SMR-TIRM consists of the same optical components found in a classic TIRM (microscope and sensor), with the differences primarily being in the location and production of the evanescent field. The coherent light source is generated from a solid-state laser coupled to a polarizing maintaining fiber that is connected to a mount with a linear filter and beam expander (see Fig. 7). The mount itself is coupled to a goniometer that can rotate 360° around the sample. The beam enters a semispherical prism such that all angles of incidence are identical regardless of the azimuthal angle direction. Variation of the azimuthal angle direction facilitates experimental collection of any arbitrary angle of morphology for a single particle. Experimental noise is then significantly reduced because mapping of different angles can be conducted on a single particle, thereby eliminating any variations inherent to an ensemble of particles.

Beyond mapping, an ultra-microscopy technique such as variable azimuthal angle SMR-TIRM expands possibilities beyond the measurement of interaction energy landscapes. For instance, our team has begun to measure and interpret morphologies from deformable particles (i.e., red blood cells) adhered to the boundary along which the evanescent wave is traveling. These experiments have revealed indeed that scattering morphology depends on the deformation state. Obtaining scattering morphologies with incident beams at a systematically varied azimuthal angle appears to be a viable avenue for obtaining the local shape of the particle as it deforms. This information could have wide-ranging implications for obtaining a detailed view of red blood cell adhesion.

In conjunction with experimental techniques for tracking particle motion, there has also been significant effort in utilizing simulations to interpret the motion of an anisotropic particle very near a boundary. Essentially, these efforts seek to determine what physiochemical features of the anisotropic particle system play a role in dictating dynamics. Such efforts have considered particles both in the absence and in the presence of fields. Our own efforts in this area initially sought to utilize the position observations as simulated with Brownian dynamics to calculate the potential energy landscape of the particle itself.[176,177] This connection is crucial to the development of SMR-TIRM because one utilizes independent measurements of position and orientation to calculate potential energy in TIRM.

First, our work found that particle properties could be obtained from fitting the potential energy landscape obtained via observation of a Janus particle's position and orientation. Yet, even though particle properties could be determined, we found that approximately 5× to 10× more observations would be required. For instance, 50 000 TIRM observations of particle position are typically required to resolve the potential energy profile for energies

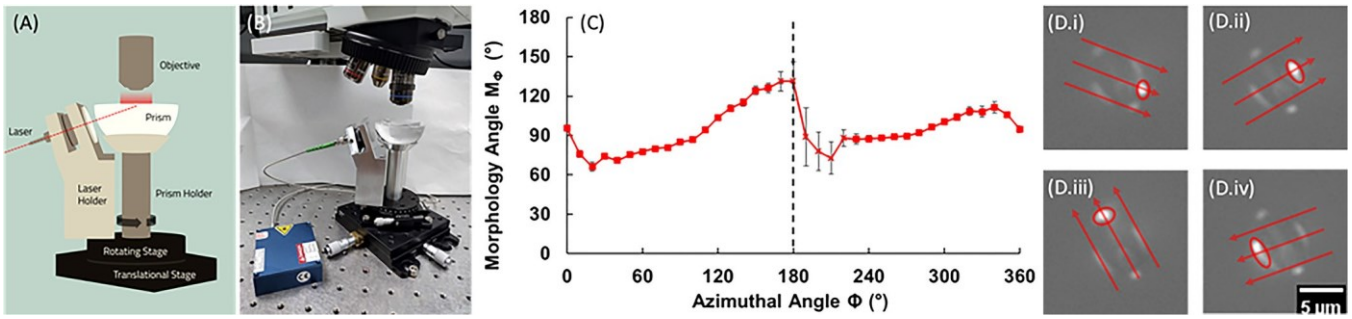

FIG. 7. SMR-TIRM with azimuthally adjustable incident beam. (a) and (b) The apparatus consists of the typical optical components found in TIRM (linearly polarized incident beam, objective), but also a hemispherical prism and rotational stage allowing for scattering morphology mapping at any azimuthal angle of a fixed particle. (c) Example data from an experiment in which a single ellipsoid was fixed to the boundary and the morphology angle was measured as a function of incident beam azimuthal angle. (d) Combination SMR-TIRM and bright-field images of an ellipsoid at angles (d.i) 144°, (d.ii) 94°, (d.iii) 4°, and (d.iv) 294°.

<6 kT of a single isotropic particle. Our work on a Janus particle, though, found that approximately 500 000 to 1 000 000 observations would be required to solve the potential energy landscape with a similar energy range. This requirement arises from the additional degree of freedom in the Janus particle's motion, namely, the polar angle. Adding an additional degree of freedom requires a similar number of observations to be spread across the range being considered. Follow-up work that considered the impact of cap weight on the dynamics of a Janus particle came to similar conclusions regarding the relationship between observations and potential energy landscape. We found the cap to have a profound impact on dynamics for experimentally relevant conditions for a Janus particle near a wall.

V. OUTLOOK AND CHALLENGES

Although the field of anisotropic colloids is quite mature, there remain burgeoning areas for growth. Although there have been some examples of large-scale production of anisotropic particles,[178] there continues to be a need for economical and scalable fabrication techniques. Application of anisotropic particles, for instance Janus particles in optically responsive materials, has been somewhat limited because of current production techniques. Very recent work has demonstrated a path to producing large quantities of Janus particles.[179] These large quantities allow for the production of liquids, a precursor to coatings, with field responsive optical properties. Health is another area that would significantly benefit from large-scale production of anisotropic particles. For example, synthetic feedstocks of platelets would benefit the available supply of synthetic blood, yet there are limited large-scale production methods for platelets or other biological cell substitutes.

Another opportunity for growth in this area is in the development of the sensing, control, and feedback mechanisms that can be designed into particles.[180] Although, as described above, there has been significant recent improvement in the ability to control the dynamics of anisotropic particles, there remain key gaps in capability. For instance, recent work has shown promise in the navigation of complex environments by anisotropic colloids, many of those examples relied on an external field to control the motion, a chemical that would not be amenable to many applications, have trajectories that are simple, or the need for the fluid to be simple. Further, there are excellent recent examples that combine many of these features into a microdevice.[181] As has been noted previously, one key motivation for studying the dynamics of anisotropic colloids when near a boundary is how well they serve as analogs to microorganisms. This has proven to be true for many instances, such as phagocytosis, biodistribution, and guiding immune responses,[182–184] but one major difference that remains between existing active systems and microorganisms is that of chemical responsiveness. Microscale objects in nature often control the magnitude or direction of dynamics with chemical responses. However, there remain very few robust examples of similar strategies with synthetic particles.

Besides the two areas noted above, other current challenges include evaluating the potential of significantly improved computing power and machine learning as applied to particle–particle interactions or particle–fluid interactions to establish a better understanding of bulk behavior in particle systems. Further pushing the boundary of visualization in concentrated systems is also a current challenge. In principle, one potential solution could be via the use of SMR-TIRM with concentrated particles that share the same refractive index (RI) as the continuous phase. Adding "probe particles" with a different RI, thereby scattering light, among the RI matched particles would be one avenue to track and further analyze the influence of neighboring particles in the vicinity of surface interactions. Regardless of these challenges, the field of fabrication, assembly, and application of anisotropic particles near a boundary remains exciting and valuable.

ACKNOWLEDGMENTS

This work was supported by the National Science Foundation CAREER Award, NSF No. 2023525. The authors thank Dr. Aidin Rashidi for help in producing Fig. 4 and Mr. John Mays for help in producing Fig. 7.

AUTHOR DECLARATIONS

Conflict of Interest

The authors have no conflicts to disclose.

DATA AVAILABILITY

The data that support the findings of this study are available from the corresponding author upon reasonable request.

REFERENCES

[1]X. Qi, C. Vetter, A. C. Harper, and V. J. Gelling, Prog. Org. Coatings 63, 345–351 (2008).

[2]E. D. Co and A. G. Marangoni, Adv. Colloid Interface Sci. 273, 102035 (2019).

[3]M. Bosma, R. Brinkhuis, J. Coopmans, and B. Reuvers, Prog. Org. Coatings 55, 97–104 (2006).

[4]G. Ferraro, E. Fratini, R. Rausa, P. Fiaschi, and P. Baglioni, Energy Fuels 30, 9859–9866 (2016).

[5]A. V. Buys, M.-J. Van Rooy, P. Soma, D. Van Papendorp, B. Lipinski, and E. Pretorius, Cardiovasc. Diabetol. 12, 25 (2013).

[6]J. Sun, X.-B. Zuo, S. Fang, H.-N. Xu, J. Chen, Y.-C. Meng, and T. Chen, J. Texture Stud. 48, 241–248 (2017).

[7]M. J. Wilson, L. Wilson, and I. Patey, Clay Miner. 49, 147–164 (2014).

[8]B. P. Binks, J. H. Clint, G. Mackenzie, C. Simcock, and C. P. Whitby, Langmuir 21, 8161–8167 (2005).

[9]M. Drechsler "Electron and Optical Microscopy" (Bavarian Polymer Institute (BPI) Keylab, University of Bayreuth Universitaetsstr., 2014).

[10]M. Diaz, L. Sayavedra, A. Atter, M. J. Mayer, S. Saha, W. Amoa-Awua, and A. Narbad, Int. J. Syst. Evol. Microbiol. 70, 3012–3017 (2020).

[11]F. Li, D. P. Josephson, and A. Stein, Angew. Chem. Int. Ed. 50, 360–388 (2011).

[12]J. J. Juárez and M. A. Bevan, J. Chem. Phys. 131, 134704 (2009).

[13]F. Ma, D. T. Wu, and N. Wu, J. Am. Chem. Soc. 135, 7839–7842 (2013).

[14]S. O. Lumsdon, E. W. Kaler, and O. D. Velev, Langmuir 20, 2108–2116 (2004).
[15]W. D. Ristenpart, I. A. Aksay, and D. A. Saville, Phys. Rev. E 69, 021405 (2004).
[16]Y. Solomentsev, M. Böhmer, and J. L. Anderson, Langmuir 13, 6058–6068 (1997).
[17]D. C. Prieve, P. J. Sides, and C. L. Wirth, Curr. Opin. Colloid Interface Sci. 15, 160–174 (2010). [18]
X. Xu, G. Friedman, K. D. Humfeld, S. A. Majetich, and S. A. Asher, Adv. Mater. 13, 1681–1684 (2001).
[19]K. H. Li and B. B. Yellen, Appl. Phys. Lett. 97, 083105 (2010). [20]J. W. Swan, J. L. Bauer, Y. Liu, and E. M. Furst, Soft Matter 10, 1102–1109 (2014).
[21]D. Du and S. L. Biswal, Phys. Rev. E 90, 033310 (2014). [22]T. W. Long, U. M. Córdova-Figueroa, and I. Kretzschmar, Langmuir 35, 8121–8130 (2019).
[23]J. L. Anderson and D. C. Prieve, Sep. Purif. Methods 13, 67–103 (1984).
[24]J. P. Ebel, J. L. Anderson, and D. C. Prieve, Langmuir 4, 396–406 (1988). [25]A. Kar, R. Guha, N. Dani, D. Velegol, and M. Kumar, Langmuir 30, 793–799 (2014).
[26]R. Piazza and A. Parola, J. Phys.: Condens. Matter 20, 153102 (2008). [27]H.-R. Jiang, H. Wada, N. Yoshinaga, and M. Sano, Phys. Rev. Lett. 102, 208301 (2009).
[28]A. Parola and R. Piazza, Eur. Phys. J. E 15, 255–263 (2004).
[29]
Z. Li, L. Bai, C. Zhou, X. Yan, L. Mair, A. Zhang, L. Zhang, and W. Wang, Part. Part. Syst. Charact. 34, 1600277 (2017).
[30]
D. Zhou, Y. Gao, J. Yang, Y. C. Li, G. Shao, G. Zhang, T. Li, and L. Li, Adv. Sci. 5, 1800122 (2018).
[31]C. Zhou, L. Zhao, M. Wei, and W. Wang, ACS Nano 11, 12668–12676 (2017).
[32]P. Kumnorkaew, Y.-K. Ee, N. Tansu, and J. F. Gilchrist, Langmuir 24, 12150–12157 (2008). [33]
N. Denkov, O. Velev, P. Kralchevski, I. Ivanov, H. Yoshimura, and K. Nagayama, Langmuir 8, 3183–3190 (1992).
[34]H. Hu and R. G. Larson, J. Phys. Chem. B 110, 7090–7094 (2006). [35]R. W. O'Brien and L. R. White, J. Chem. Soc., Faraday Trans. 2 74, 1607 (1978). [36]
T. B. Jones, Electromechanics of Particles (Cambridge University Press, 2005).
[37]J. D. Hoggard, P. J. Sides, and D. C. Prieve, Langmuir 24, 2977–2982 (2008).
[38]
J. Kim, S. A. Guelcher, S. Garoff, and J. L. Anderson, Adv. Colloid Interface Sci. 96, 131–142 (2002). [39]T. D. Edwards and M. A. Bevan, Langmuir 30, 10793–10803 (2014).
[40]
A. Spatafora-Salazar, D. M. Lobmeyer, L. H. P. Cunha, K. Joshi, and S. L. Biswal, Soft Matter 17, 1120–1155 (2021). [41]M. Wang, L. He, and Y. Yin, Mater. Today 16, 110–116 (2013).
[42]
C. Ludwig, Diffusion Zwischen Ungleich Erwärmten Orten Gleich Zusammengesetzter Lösung (Aus der KK Hof-und Staatsdruckerei, in Commission bei W. Braumüller, 1856).
[43]C. Soret, Arch. Sci. Phys. Nat. Geneve 2, 48 (1879).
[44]B. G. Prevo and O. D. Velev, Langmuir 20, 2099–2107 (2004). [45]S. C. Glotzer and M. J. Solomon, Nat. Mater. 6, 557–562 (2007).
[46]
M. Das, L. Chambon, Z. Varga, M. Vamvakaki, J. W. Swan, and G. Petekidis, Soft Matter 17, 1232–1245 (2021).
[47]
S. Ebbens, D. A. Gregory, G. Dunderdale, J. R. Howse, Y. Ibrahim, T. B. Liverpool, and R. Golestanian, Europhys. Lett. 106, 58003 (2014). [48]P. D. Cobb and J. E. Butler, J. Chem. Phys. 123, 054908 (2005). [49]A. M. Menzel, Phys. Rep. 554, 1–45 (2015).
[50]
Y. Man, E. Kucukal, R. An, Q. D. Watson, J. Bosch, P. A. Zimmerman, J. A. Little, U. A. Gurkan, and U. A. Gurkan, Lab Chip 20, 2086–2099 (2020).
[51]
R. Huisjes, A. Bogdanova, W. W. van Solinge, R. M. Schiffelers, L. Kaestner, and R. van Wijk, Front. Physiol. 9, 1 (2018). [52]D. C. Rees, T. N. Williams, and M. T. Gladwin, Lancet 376, 2018–2031 (2010).
[53]
N. D. Burrows, A. M. Vartanian, N. S. Abadeer, E. M. Grzincic, L. M. Jacob, W. Lin, J. Li, J. M. Dennison, J. G. Hinman, and C. J. Murphy, J. Phys. Chem. Lett. 7, 632–641 (2016).
[54]H. K. Bisoyi and Q. Li, Chem. Rev. 122, 4887–4926 (2021). [55]L. C. Hsiao, I. Saha-Dalal, R. G. Larson, and M. J. Solomon, Soft Matter 13, 9229–9236 (2017).
[56]
M. Voggenreiter, J. Roller, J. Geiger, L. Ebner, A. Zumbusch, and J.-M. Meijer, Langmuir 36, 13087–13095 (2020).
[57]J. D. Forster, J.-G. Park, M. Mittal, H. Noh, C. F. Schreck, C. S. O'Hern, H. Cao, E. M. Furst, and E. R. Dufresne, ACS Nano 5, 6695–6700 (2011). [58]H. Y. Koo, D. K. Yi, S. J. Yoo, and D.-Y. Kim, Adv. Mater. 16, 274–277 (2004).
[59]J.-M. Meijer and J. J. Crassous, Small 14, 1802049 (2018). [60]C. C. Ho, A. Keller, J. A. Odell, and R. H. Ottewill, Colloid Polym. Sci. 271, 469–479 (1993).
[61]B. Madivala, J. Fransaer, and J. Vermant, Langmuir 25, 2718–2728 (2009). [62]S. Coertjens, P. Moldenaers, J. Vermant, and L. Isa, Langmuir 30, 4289–4300 (2014). [63]
J. P. Singh, P. P. Lele, F. Nettesheim, N. J. Wagner, and E. M. Furst, Phys. Rev. E 79, 050401 (2009).
[64]P. J. Beltramo, D. Schneider, G. Fytas, and E. M. Furst, Phys. Rev. Lett. 113, 205503 (2014).
[65]J. Yan, A. Rashidi, and C. L. Wirth, Colloids Surf., A 606, 125384 (2020). [66]J. A. Ferrar, L. Pavlovsky, E. Viges, Y. Liu, and M. J. Solomon, AIChE J. 64, 697–707 (2018). [67]S. Trevenen and P. J. Beltramo, J. Colloid Interface Sci. 583, 385–393 (2021).
[68]
Z. Zhang, P. Pfleiderer, A. B. Schofield, C. Clasen, and J. Vermant, J. Am. Chem. Soc. 133, 392–395 (2011).
[69]
D. Zerrouki, B. Rotenberg, S. Abramson, J. Baudry, C. Goubault, F. Leal-Calderon, D. J. Pine, and J. Bibette, Langmuir 22, 57–62 (2006).
[70]
Y. Wang, Y. Wang, D. R. Breed, V. N. Manoharan, L. Feng, A. D. Hollingsworth, M. Weck, and D. J. Pine, Nature 491, 51–55 (2012). [71]D. Zerrouki, J. Baudry, D. Pine, P. Chaikin, and J. Bibette, Nature 455, 380–382 (2008). [72]
L. Xu, W. Ma, L. Wang, C. Xu, H. Kuang, and N. A. Kotov, Chem. Soc. Rev. 42, 3114 (2013). [73]
H. R. Sheu, M. S. El-Aasser, and J. W. Vanderhoff, J. Polym. Sci., Part A: Polym. Chem. 28, 653–667 (1990).
[74]
H. R. Sheu, M. S. El-Aasser, and J. W. Vanderhoff, J. Polym. Sci., Part A: Polym. Chem. 28, 629–651 (1990).
[75]J.-W. Kim, R. J. Larsen, and D. A. Weitz, J. Am. Chem. Soc. 128, 14374–14377 (2006).
[76]W. Lu, M. Chen, and L. Wu, J. Colloid Interface Sci. 328, 98–102 (2008). [77]K. Yoon, D. Lee, J. W. Kim, J. Kim, and D. A. Weitz, Chem. Commun. 48, 9056 (2012).
[78]S. Wang, F. Ma, H. Zhao, and N. Wu, ACS Appl. Mater. Interfaces 6, 4560–4569 (2014).

[79]A. Kuijk, A. van Blaaderen, and A. Imhof, J. Am. Chem. Soc. 133, 2346–2349 (2011).

[80]A. K. Pearce, T. R. Wilks, M. C. Arno, and R. K. O'Reilly, Nat. Rev. Chem. 5, 21–45 (2021). [81]S. L. Tao, K. Popat, and T. A. Desai, Nat. Protoc. 1, 3153–3158 (2006).

[82] I. Sakellari, X. Yin, M. L. Nesterov, K. Terzaki, A. Xomalis, and M. Farsari, Adv. Opt. Mater. 5, 1700200 (2017).

[83] A. Nishiguchi, F. Shima, S. Singh, M. Akashi, and M. Moeller, Biomacromolecules 21, 2043–2048 (2020). [84]H. Takei and N. Shimizu, Langmuir 13, 1865–1868 (1997).

[85] K. J. Robbie and M. J. Brett, US6206065B1 (July 30, 1997).

[86]K. Robbie, J. Vac. Sci. Technol., B 16, 1115 (1998).

[87]A. B. Pawar and I. Kretzschmar, Langmuir 24, 355–358 (2008).

[88]A. B. Pawar and I. Kretzschmar, Langmuir 25, 9057–9063 (2009). [89]Z. He and I. Kretzschmar, Langmuir 29, 15755–15761 (2013).

[90] A. Rashidi, M. W. Issa, I. T. Martin, A. Avishai, S. Razavi, and C. L. Wirth, ACS Appl. Mater. Interfaces 10, 30925–30929 (2018).

[91] I. Buttinoni, J. Bialké, F. Kümmel, H. Löwen, C. Bechinger, and T. Speck, Phys. Rev. Lett. 110, 238301 (2013).

[92]L. Hong, S. Jiang, and S. Granick, Langmuir 22, 9495–9499 (2006). [93]B. Liu, W. Wei, X. Qu, and Z. Yang, Angew. Chem. 120, 4037–4039 (2008). [94]

A. Kirillova, G. Stoychev, L. Ionov, K.-J. Eichhorn, M. Malanin, and A. Synytska, ACS Appl. Mater. Interfaces 6, 13106–13114 (2014).

[95] A. C. de Leon, B. J. Rodier, Q. Luo, C. M. Hemmingsen, P. Wei, K. Abbasi, R. Advincula, and E. B. Pentzer, ACS Nano 11, 7485–7493 (2017). [96]B. Rodier, A. De Leon, C. Hemmingsen, and E. Pentzer, ACS Macro Lett. 6, 1201–1206 (2017).

[97] A. A. Shah, B. Schultz, W. Zhang, S. C. Glotzer, and M. J. Solomon, Nat. Mater. 14, 117–124 (2015).

[98] A. A. Shah, B. Schultz, K. L. Kohlstedt, S. C. Glotzer, and M. J. Solomon, Langmuir 29, 4688–4696 (2013).

[99]J. G. Lee, A. Al Harraq, K. J. M. Bishop, and B. Bharti, J. Phys. Chem. B 125, 4232–4240 (2021). [100]

T. J. Woehl, K. L. Heatley, C. S. Dutcher, N. H. Talken, and W. D. Ristenpart, Langmuir 30, 4887–4894 (2014).

[101]F. Ma, S. Wang, D. T. Wu, and N. Wu, Proc. Natl. Acad. Sci. 112, 6307–6312 (2015). [102]

C. S. Dutcher, T. J. Woehl, N. H. Talken, and W. D. Ristenpart, Phys. Rev. Lett. 111, 128302 (2013).

[103]F. Ma, S. Wang, H. Zhao, D. T. Wu, and N. Wu, Soft Matter 10, 8349–8357 (2014).

[104]J. Gong and N. Wu, Langmuir 33, 5769–5776 (2017).

[105]C. L. Wirth and S. H. Nuthalapati, Phys. Rev. E 94, 042614 (2016).

[106]M. Rath, J. Weaver, M. Wang, and T. Woehl, Langmuir 37, 9346–9355 (2021).

[107]J. R. Maestas, F. Ma, N. Wu, and D. T. Wu, ACS Nano 15, 2399–2412 (2021). [108]

X. Zhu, Y. Gao, R. Mhana, T. Yang, B. L. Hanson, X. Yang, J. Gong, and N. Wu, Langmuir 37, 9151–9161 (2021).

[109]F. Ma, X. Yang, H. Zhao, and N. Wu, Phys. Rev. Lett. 115, 208302 (2015). [110]S. Gangwal, O. J. Cayre, M. Z. Bazant, and O. D. Velev, Phys. Rev. Lett. 100, 058302 (2008).

[111]S. Gangwal, A. Pawar, I. Kretzschmar, and O. D. Velev, Soft Matter 6, 1413 (2010).

[112]M. S. Kilic and M. Z. Bazant, Electrophoresis 32, 614–628 (2011). [113]M. Z. Bazant, M. S. Kilic, B. D. Storey, and A. Ajdari, New J. Phys. 11, 075016 (2009).

[114] P. Bahukudumbi, W. N. Everett, A. Beskok, M. A. Bevan, G. H. Huff, D. Lagoudas, and Z. Ounaies, Appl. Phys. Lett. 90, 224102 (2007).

[115]A. Castellanos and A. Ramos, J. Phys. D: Appl. Phys 36, 2584–2597 (2003).

[116]D. Du, E. Hilou, and S. L. Biswal, Soft Matter 14, 3463–3470 (2018). [117]J. Byrom and S. L. Biswal, Soft Matter 9, 9167 (2013).

[118] T. Yang, B. Sprinkle, Y. Guo, J. Qian, D. Hua, A. Donev, D. W. M. Marr, and N. Wu, Proc. Natl. Acad. Sci. 117, 18186–18193 (2020). [119]A. Al Harraq, J. G. Lee, and B. Bharti, Sci. Adv. 6, eaba5337 (2020).

[120] J. A. Victoria-Camacho, R. A. DeLaCruz-Araujo, I. Kretzschmar, and U. M. Córdova-Figueroa, Soft Matter 16, 2460–2472 (2020). [121]

G. I. Vega-Bellido, R. A. DeLaCruz-Araujo, I. Kretzschmar, and U. M. Córdova-Figueroa, Soft Matter 15, 4078–4086 (2019). [122]

K. Han, C. W. Shields, N. M. Diwakar, B. Bharti, G. P. López, and O. D. Velev, Sci. Adv. 3, e1701108 (2017).

[123]K. Han, C. W. Shields, B. Bharti, P. E. Arratia, and O. D. Velev, Langmuir 36, 7148–7154 (2020). [124]

T. Yang, A. Tomaka, T. O. Tasci, K. B. Neeves, N. Wu, and D. W. M. Marr, Sci. Robot. 4, eaaw9525 (2019).

[125]T. Yang, T. O. Tasci, K. B. Neeves, N. Wu, and D. W. M. Marr, Langmuir 33, 5932–5937 (2017). [126]S. J. Ebbens and J. R. Howse, Soft Matter 6, 726 (2010).

[127] J. R. Howse, R. A. L. Jones, A. J. Ryan, T. Gough, R. Vafabakhsh, andR. Golestanian, Phys. Rev. Lett. 99, 8 (2007). [128]

W. F. Paxton, K. C. Kistler, C. C. Olmeda, A. Sen, S. K. St. Angelo, Y. Cao, T. E. Mallouk, P. E. Lammert, and V. H. Crespi, J. Am. Chem. Soc. 126, 13424–13431 (2004).

[129]W. F. Paxton, A. Sen, and T. E. Mallouk, Chem. A Eur. J. 11, 6462–6470 (2005). [130]

S. Das, Z. Jalilvand, M. N. Popescu, W. E. Uspal, S. Dietrich, and I. Kretzschmar, Langmuir 36, 7133–7147 (2020). [131]

I. Buttinoni, G. Volpe, F. Kümmel, G. Volpe, and C. Bechinger, J. Phys.: Condens. Matter 24, 284129 (2012).

[132] F. Kümmel, B. ten Hagen, R. Wittkowski, I. Buttinoni, R. Eichhorn, G. Volpe, H. Löwen, and C. Bechinger, Phys. Rev. Lett. 110, 198302 (2013).

[133] J. Palacci, S. Sacanna, A. P. Steinberg, D. J. Pine, and P. M. Chaikin, Science 339, 936–940 (2013). [134]

L. Alvarez, M. A. Fernandez-Rodriguez, A. Alegria, S. Arrese-Igor, K. Zhao, M. Kröger, and L. Isa, Nat. Commun. 12, 4762 (2021).

[135]Y. Ji, X. Lin, H. Zhang, Y. Wu, J. Li, and Q. He, Angew. Chem. Int. Ed. 58, 4184–4188 (2019). [136]

Z. Wang, Z. Wang, J. Li, S. T. H. Cheung, C. Tian, S.-H. Kim, G.-R. Yi, E. Ducrot, and Y. Wang, J. Am. Chem. Soc. 141, 14853–14863 (2019).
[137]C. W. Shields, K. Han, F. Ma, T. Miloh, G. Yossifon, and O. D. Velev, Adv. Funct. Mater. 28, 1803465 (2018).
[138]N. Tanjeem, M. B. Minnis, R. C. Hayward, and C. W. Shields, Adv. Mater. 34, 2105758 (2022). [139]C. W. Shields and O. D. Velev, Chem 3, 539–559 (2017).
[140]V. Carniello, B. W. Peterson, H. C. van der Mei, and H. J. Busscher, Adv. Colloid Interface Sci. 261, 1–14 (2018).
[141]H. Brenner, Chem. Eng. Sci. 16, 242–251 (1961).
[142]H. Brenner, J. Colloid Sci. 20, 104–122 (1965).
[143]M. A. Bevan and D. C. Prieve, Langmuir 16, 9274–9281 (2000).
[144]R. J. Oetama and J. Y. Walz, J. Chem. Phys. 124, 164713 (2006).
[145]C. C. Chio and Y.-L. S. Tse, Langmuir 36, 9412–9423 (2020).
[146]D. C. Prieve, Adv. Colloid Interface Sci. 82, 93–125 (1999). [147]M. A. Bevan and S. L. Eichmann, Curr. Opin. Colloid Interface Sci. 16, 149–157 (2011). [148]S. Rakshit and S. Sivasankar, Phys. Chem. Chem. Phys. 16, 2211 (2014).
[149]M. Diao, E. Taran, S. Mahler, T. A. H. Nguyen, and A. V. Nguyen, Colloids Surf., B 115, 229–236 (2014).
[150]G. C. L. Wong, J. D. Antani, P. Lele, J. Chen, B. Nan, M. J. Kühn, A. Persat, J.-L. Bru, N. M. Høyland-Kroghsbo, A. Siryaporn, J. Conrad, F. Carrara, Y. Yawata, R. Stocker, Y. Brun, G. Whitfield, C. Lee, J. de Anda, W. C. Schmidt, R. Golestanian, G. A. O'Toole, K. Floyd, F. Yildiz, S. Yang, F. Jin, M. Toyofuku, L. Eberl, N. Nobuhiko, L. Zacharoff, M. Y. El-Naggar, S. E. Yalcin, N. Malvankar, M. D. Rojas-Andrade, A. Hochbaum, J. Yan, H. A. Stone, N. S. Wingreen, B. Bassler, Y. Wu, H. Xu, K. Drescher, and J. Dunkel, Phys. Biol. 18, 051501 (2021). [151]M. Stroobach, L. Haya, and M. Fenech, Med. Eng. Phys. 69, 100–108 (2019). [152]H. Ye, Z. Shen, and Y. Li, IEEE Trans. Nanotechnol. 17, 407–411 (2018).
[153]E. Kucukal, A. Ilich, N. S. Key, J. A. Little, and U. A. Gurkan, Am. J. Hematol. 93, 1050–1060 (2018).
[154]E. Kucukal, Y. Man, E. Quinn, N. Tewari, R. An, A. Ilich, N. S. Key, J. A. Little, and U. A. Gurkan, Blood Adv. 4, 3688–3698 (2020).
[155]S. Sharma, Y. A. Jaimes-Lizcano, R. B. McLay, P. C. Cirino, and J. C. Conrad, Langmuir 32, 5422–5433 (2016).
[156]J. Schwarz-Linek, J. Arlt, A. Jepson, A. Dawson, T. Vissers, D. Miroli, T. Pilizota, V. A. Martinez, and W. C. K. Poon, Colloids Surf., B 137, 2–16 (2016).
[157]R. B. McLay, H. N. Nguyen, Y. A. Jaimes-Lizcano, N. K. Dewangan, S. Alexandrova, D. F. Rodrigues, P. C. Cirino, and J. C. Conrad, Langmuir 34, 1133–1142 (2018).
[158]S. Perni, E. C. Preedy, and P. Prokopovich, Adv. Colloid Interface Sci. 206, 265–274 (2014). [159]N. Figueroa-Morales, A. Rivera, R. Soto, A. Lindner, E. Altshuler, and É Clément, Sci. Adv. 6, eaay0155 (2020).
[160]Y. Deng, D. P. Papageorgiou, H.-Y. Chang, S. Z. Abidi, X. Li, M. Dao, and G. E. Karniadakis, Biophys. J. 116, 360–371 (2019).
[161]E. Kucukal, Y. Man, A. Hill, S. Liu, A. Bode, R. An, J. Kadambi, J. A. Little, and U. A. Gurkan, Am. J. Hematol. 95, 1246–1256 (2020).
[162]E. Kucukal, J. A. Little, and U. A. Gurkan, Integr. Biol. 10, 194–206 (2018).
[163]Y. Alapan, J. A. Little, and U. A. Gurkan, Sci. Rep. 4, 7173 (2014). [164]D. A. Fedosov, B. Caswell, and G. E. Karniadakis, Biophys. J. 100, 2084–2093 (2011).
[165]L. Lu, Z. Li, H. Li, X. Li, P. G. Vekilov, and G. E. Karniadakis, Sci. Adv. 5, eaax3905 (2019). [166]D. P. Papageorgiou, S. Z. Abidi, H.-Y. Chang, X. Li, G. J. Kato, G. E. Karniadakis, S. Suresh, and M. Dao, Proc. Natl. Acad. Sci. 115, 9473–9478 (2018).
[167]J. Crocker, D. Grier, J. Crocker, and D. Grier, J. Colloid Interface Sci. 179, 298 (1996). [168]D. G. Grier, Github (2016); available at https://github.com/davidgrier/features/.
[169]D. Blair and E. R. Dufresne (n.d.); available at https://site.physics.georgetown.edu/matlab/.
[170]F. C. Cheong and D. G. Grier, Opt. Express 18, 6555 (2010).
[171]D. C. Prieve and J. Y. Walz, Appl. Opt. 32, 1629 (1993). [172]D. C. Prieve and N. A. Frej, Langmuir 6, 396–403 (1990).
[173]A. Doicu, A. A. Vasilyeva, D. S. Efremenko, C. L. Wirth, and T. Wriedt, J. Mod. Opt. 66, 1139–1151 (2019). [174]A. Rashidi, S. Domínguez-Medina, J. Yan, D. S. Efremenko, A. A. Vasilyeva, A. Doicu, T. Wriedt, and C. L. Wirth, Langmuir 36, 13041–13050 (2020). [175]J. Yan, D. S. Efremenko, A. A. Vasilyeva, A. Doicu, T. Wriedt, and C. Wirth, Comput. Math. Model. 32, 86–93 (2021).
[176]A. Rashidi and C. L. Wirth, J. Chem. Phys. 147, 224906 (2017).
[177]A. Rashidi, S. Razavi, and C. L. Wirth, Phys. Rev. E 101, 042606 (2020).
[178]J. L. Perry, K. P. Herlihy, M. E. Napier, and J. M. DeSimone, Acc. Chem. Res. 44, 990–998 (2011). [179]J. F. Gilchrist, in AIChE Annual Meeting 01C Plenary Session (American Institute of Chemical Engineers, 2021).
[180]J. Zhang, J. Yang, Y. Zhang, and M. A. Bevan, Sci. Adv. 6, eabd6716 (2020).
[181]K. Han, C. W. Shields, and O. D. Velev, Adv. Funct. Mater. 28, 1705953 (2018). [182]J. J. Moon, B. Huang, and D. J. Irvine, Adv. Mater. 24, 3724–3746 (2012).
[183]S. Shukla, F. J. Eber, A. S. Nagarajan, N. A. DiFranco, N. Schmidt, A. M. Wen, S. Eiben, R. M. Twyman, C. Wege, and N. F. Steinmetz, Adv. Healthcare Mater. 4, 874–882 (2015).
[184]J. A. Champion and S. Mitragotri, Proc. Natl. Acad. Sci. 103, 4930–4934 (2006). [185]S. Coertjens, R. De Dier, P. Moldenaers, L. Isa, and J. Vermant, Langmuir 33, 2689–2697 (2017).
[186]F. Ma, S. Wang, L. Smith, and N. Wu, Adv. Funct. Mater. 22, 4334–4343 (2012).